Metal chelation by the common 2-amino-2-deoxy-, 2-*N*-acetylamino-2-deoxy-, and 2-deoxy-hexoses†

Thomas Schwarz, David Heß and Peter Klüfers*

Received 10th February 2010, Accepted 9th April 2010
First published as an Advance Article on the web 11th May 2010
DOI: 10.1039/c002711a

The chelating properties of the common aldohexoses D-glucose, D-mannose, and D-galactose are characteristically modified in 2-substituted derivatives. The 2-amino-2-deoxy-aldohexoses provide mono- and bis-metallisable anionic ligands after their reaction with metal probes of the $Pd^{II}N_2$ type (N_2 = bidentate nitrogen ligand). The 2-amino function reliably participates in metal binding of the, mostly pyranoidic, carbohydrate chelators. Acetylation of the amino function yields the biologically important 2-*N*-acetylamino-2-deoxy-hexoses (GlcNAc, ManNAc, and GalNAc). On reaction with the palladium probe, the metal-binding properties of the deprotonated acetylamino function depends on the steric requirements introduced by the acetyl residue which is forced into a coplanar arrangement with the chelate ring. In the two 2-deoxy-aldohexoses, 2-deoxy-*arabino*-D-hexose (the 2-deoxy derivative of both D-glucose and D-mannose, '2-deoxy-glucose') and 2-deoxy-*lyxo*-D-hexose ('2-deoxy galactose'), the 2-position cannot contribute to metal binding. As a result, furanose-1,3 chelation becomes an important metal-binding mode. Due to the decreased acidity of the 2-deoxy-glycose's 1-hydroxy function, monometallation also takes place at the pyranose's 3,4-site.

Introduction

The 2-amino-2-deoxy derivatives of the common aldohexoses D-glucose, D-mannose, and D-galactose ('glucosamine', 'galactosamine', 'mannosamine') as well as their *N*-acetyl derivatives ('GlcNAc', 'GalNAc', 'ManNAc') are ubiquitous biomolecules with a variety of physiological functions. Moreover, particularly the glucose derivatives, which are produced in large quantities from the workup of chitin, are available as a renewable feedstock. Since the anomeric centres of the parent glycoses are not affected by the (acetyl)amination, all these substances are reducing sugars. Thus, pairs of furanose and pyranose anomers as well as the minor open-chain forms, may be accessible in the course of a chemical reaction. Laying the focus on metal chelation, the amino- and the *N*-acetylamino-hexoses are treated differently in the literature. The glycosamines are known to be ligands. Details of their binding sites, however, are hardly known due to methodological problems. Thus, neither crystal-structure analyses nor exhaustive NMR-spectroscopical work is available for these ligands. Instead, potentiometric, polarographic, and CD- and UV/Vis-spectroscopic investigations have been published as well as ^{1}H NMR results.[1-7] In a platinum(IV) complex of D-glucosamine, complexation of solely the α-pyranose has been formulated but not all coupling constants were resolved to confirm the assignment.[8] In recent work, palladium complexes of non-reducing chitosan model glycosides have been investigated by contemporary methods. As a result, five-membered chelate rings with chitosan's vicinal aminoalcohol function were formulated.[9,10] A literature survey for the *N*-acetylamino-hexoses produced a different outcome. To our knowledge, none of these have ever been regarded as capable of metal chelation, a reason for which may be that the *N*-acetylamino function's ligand properties have been judged as parallelling its acid–base behaviour. In an aqueous medium, neither protonation nor deprotonation is of any significance. Being thus 'silent' in terms of metal binding, a close similarity may be assumed to the respective 2-deoxy-hexoses, another class of reducing sugars of biochemical significance. In this work, we present a study on the chelating properties of these three groups of 2-modified aldose derivatives. To probe the metal-binding sites, $Pd^{II}N_2$-type fragments which were investigated recently to unravel the bidentate metal-binding sites of the parent glycoses were used.[11]

Results and discussion

Nomenclature

Ligand abbreviations follow IUPAC usage. Thus, Glc denotes glucose, Glc*p* is used for glucopyranose, Glc*p*2N denotes 2-amino-2-deoxy glucopyranose, Glc*p*2NAc denotes 2-*N*-acetylamino-2-deoxy glucopyranose. The shortened biochemical usage is adapted for the *N*-acetyl derivatives if no actual isomer is addressed (GlcNAc, ManNAc, GalNAc). Deprotonated sites are treated similarly, Glc*p*2N3H$_{-1}$ thus being 3-deprotonated Glc*p*2N. The metal-binding site is specified by using the kappa convention. Hence, in total, β-D-Glc*p*2N3H$_{-1}$-κN^2,O^3 denotes 3-deprotonated 2-amino-2-deoxy-β-D-glucopyranose bidentately binding through its N2 and O3 atoms.

For the metal probes, a nomenclature introduced for the description of the so-called 'coordinating' cellulose solvents is used.[12] 'Pd-en' thus is an aqueous solution of [Pd(en)(OH)$_2$] (en = ethylenediamine).

Department of Chemistry of the Ludwig Maximilian University Munich, Butenandtstr. 5–13, D-81377, Munich, Germany. E-mail: kluef@cup.uni-muenchen.de; Fax: +49 89 2180 77407

† CCDC reference numbers 765816–765818. For crystallographic data in CIF or other electronic format see DOI: 10.1039/c002711a

2-Amino-2-deoxy-glycose (glycosamine) chelates

2-Amino-2-deoxy-D-glucose (D-glucosamine). In the anomeric equilibrium of 2-amino-2-deoxy-D-glucose (D-glucosamine) hydrochloride, the α- (*ca.* 2/3) and β-pyranose (*ca.* 1/3) are predominant; concentration values for minor isomers are not available.[13] Equimolar solutions of D-glucosamine hydrochloride in 0.3 M Pd-en adjust at a pH value of about 9. The ^{13}C NMR spectra (Fig. 1a, Table 1) revealed four products. In the two major species [Pd(en)(α-D-Glc*p*2N1H$_{-1}$-κO^1,N^2)]$^+$ (**1a**) and [Pd(en)(β-D-Glc*p*2N1H$_{-1}$-κO^1,N^2)]$^+$ (**1b**), the most acidic hydroxy function with O1 was deprotonated and part of a five-membered chelate ring. In the two minor species [Pd(en)(α-D-Glc*p*2N3H$_{-1}$-κN^2,O^3)]$^+$ (**1c**), [Pd(en)(β-D-Glc*p*2N3H$_{-1}$-κN^2,O^3)]$^+$ (**1d**), the less acidic hydroxy group with O3 was found as part of a chelate (Scheme 1). In agreement with the prevalence of five-membered chelate rings, the "coordination-induced shifts" (CISs), downfield shifts of the signals of those carbon atoms that bear a metal-binding atom, were about 10 ppm downfield for the alkoxido ligator and about 6 ppm for the amine-binding C2. The anomeric distribution in **1** is in agreement both with anomeric-effect considerations and with the fact that a *cis*-diol function is a better palladium chelator than a *trans*-diol.

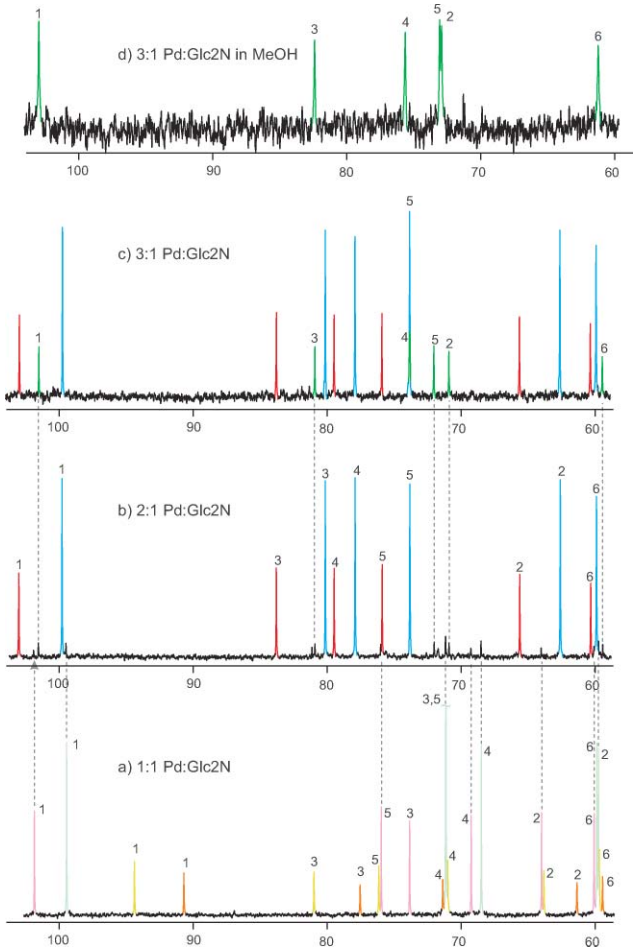

Fig. 1 ^{13}C NMR spectra of solutions of D-glucosamine hydrochloride in Pd-en. a) 1 : 1 molar ratio; light blue signals: the α anomer of [Pd(en)(D-Glc*p*2N1H$_{-1}$-κO^1,N^2)]$^+$ (**1a**), light red signals: the β anomer **1b**, orange signals (C5 coincides with C3/5 of **1a**): the α anomer of [Pd(en)(D-Glc*p*2N3H$_{-1}$-κN^2,O^3)]$^+$ (**1c**), yellowish signals: the β anomer **1d**. b) 2 : 1 molar ratio; blue signals: the α anomer of [Pd$_2$(en)$_2$(D-Glc*p*2N1,3,4H$_{-3}$-κO^1,N^2:κ$O^{3,4}$)]$^+$ (**2a**), red signals: the β anomer **2b**; small signals of species that are predominant at the 1 : 1 and the 3 : 1 molar ratio are assigned to their parent signals by dashed lines. c) 3 : 1 molar ratio; green signals: the tentative Pd$_3$ species **3**, which becomes the only species in a d) 3 : 1 solution in methanol instead of water.

1a and **1b** may be dimetallated by establishing a second chelate ring *via* O3 and O4. In fact, the two expected anomeric binuclear complexes [Pd$_2$(en)$_2$(α-D-Glc*p*2N1,3,4H$_{-3}$-κO^1,N^2:κ$O^{3,4}$)]$^+$ (**2a**) and [Pd$_2$(en)$_2$(β-D-Glc*p*2N1,3,4H$_{-3}$-κO^1,N^2:κ$O^{3,4}$)]$^+$ (**2b**) were the main constituents of solutions at the 2 : 1 molar ratio of Pd : glycosamine (Table 1; Scheme 1, middle). The ^{13}C NMR spectrum (Fig. 1b) showed a slight contamination by the signals of monometallated species and a minor species which was not present in the equimolar batches. At the still higher molar ratio of Pd : glycosamine of 3 : 1, this new species enriched the solution (Fig. 1c). Attempts to further enrich this tentative trimetallated species were successful after suppressing protolysis by replacing water with methanol (Fig. 1d). The tentative assignment of the signals and the resulting CIS values were compatible with formula **3** (Scheme 1). 2-Amino-2-deoxy-D-xylose, the des-6-hydroxymethyl derivative of 2-amino-2-deoxy-D-glucose, was expected to be unable to form such a species and, in fact, it did not. However, despite this proof, the trimetallated species needs future confirmation.

2-Amino-2-deoxy-D-mannose (D-mannosamine). The amino function's 2-axial position in D-mannosamine resulted in a simplification of the glycosamine's ligand properties since κO^1,N^2-chelation of the α-pyranose was, for steric reasons, no longer possible. An equimolar solution of D-mannosamine hydrochloride in Pd-en thus showed one major product as indicated by ^{13}C NMR spectroscopy (Table 1), the [Pd(en)(β-D-Man*p*2N1H$_{-1}$-κO^1,N^2)]$^+$ (**4a**) species. Small amounts of the minor species [Pd(en)(α-D-Man*p*2N3H$_{-1}$-κN^2,O^3)]$^+$ (**4b**) and [Pd(en)(β-D-Man*p*2N3H$_{-1}$-κN^2,O^3)]$^+$ (**4c**) completed the solution equilibrium (Scheme 2, Fig. 7 in the Appendix).

At a molar Pd : glycosamine ratio of 2 : 1, an even clearer result was obtained. Standard ^{13}C NMR spectroscopy indicated the dimetallated pyranose complex [Pd$_2$(en)$_2$(β-D-Man*p*2N1,3,4H$_{-3}$-κO^1,N^2:κ$O^{3,4}$)]$^+$ (**5**) exclusively and free of side products (Table 1, Scheme 2)—the same result that was obtained for D-mannose itself.[11] No additional species emerged in 3 : 1 batches, either in aqueous or in methanolic solution. Accordingly, simple wire models showed that the orbital directions at the nitrogen atom are not suited for the bridging bonding mode that was assigned to the trinuclear glucosamine species.

2-Amino-2-deoxy-D-galactose (D-galactosamine). Steric restrictions such as the one found for D-mannosamine were not expected for D-galactosamine. In fact, the coordination behaviour of the galactose derivative closely paralleled that of D-glucosamine. Hence, at an equimolar ratio of Pd and galactosamine, the same four-species scenario as for the glucose derivative was found spectroscopically (Table 1, Fig. 2). The main products [Pd(en)(α-D-Gal*p*2N1H$_{-1}$-κO^1,N^2)]$^+$ (**6a**) and its β derivative **6b** as well as the minor anomers [Pd(en)(α/β-D-Gal*p*2N3H$_{-1}$-κN^2,O^3)]$^+$ (**6c**,**d**) (Scheme 3) showed about the same quantities as for glucosamine. However, the similarity was limited by the fact that, in addition

Table 1 ^{13}C NMR shifts of 2-deoxy-2-amino-glycose complexes in Pd-en. $\Delta\delta$, the difference of a shift in the presence of the metal probe and the shift of the same isomer of the free glycosamine, is given if the values of the latter are accessible.

		C1	C2	C3	C4	C5	C6	glycose isomer	chelating site
1a	δ	99.4	59.8	71.2	68.5	71.2	59.9	α-D-Glc*p*2N	κO^1,N^2
	$\Delta\delta$	10.1	5.3	1.4	–1.3	–0.6	–0.6		
1b	δ	101.8	64.1	73.9	69.3	76.0	60.1	β-D-Glc*p*2N	κO^1,N^2
	$\Delta\delta$	8.9	7.2	1.7	–0.6	–0.3	–0.6		
1c	δ	90.7	61.4	77.6	71.4	71.2	59.5	α-D-Glc*p*2N	κN^2,O^3
	$\Delta\delta$	1.4	6.9	7.8	1.6	–0.6	–1.0		
1d	δ	94.4	63.9	81.0	71.1	76.2	59.8	β-D-Glc*p*2N	κN^2,O^3
	$\Delta\delta$	1.5	7.0	8.8	1.2	–0.1	–0.9		
2a	δ	99.7	62.6	80.1	77.9	73.8	59.9	α-D-Glc*p*2N	κO^1,N^2:κ$O^{3,4}$
	$\Delta\delta$	10.4	8.1	10.3	8.1	2.0	–0.6		
2b	δ	103.0	65.7	83.7	79.5	75.9	60.4	β-D-Glc*p*2N	κO^1,N^2:κ$O^{3,4}$
	$\Delta\delta$	10.1	8.8	11.6	9.6	–0.4	–0.3		
3[a]	δ	101.5	70.9	80.9	73.9	72.0	59.5	α-D-Glc*p*2N	κO^1,N^2:κN^2,O^3:κ$O^{4,6}$
	$\Delta\delta$	12.2	16.4	11.1	2.2	2.1	–1.0		
4a	δ	102.9	63.5	69.4	65.9	74.8	60.3	β-D-Man*p*2N	κO^1,N^2
	$\Delta\delta$	12.5	8.4	0.5	0.5	–0.6	0.5		
4b	δ	89.9	61.2	76.7	69.2	70.9	59.9	α-D-Man*p*2N	κN^2,O^3
	$\Delta\delta$	0.1	7.2	10.4	3.7	–0.2	0.2		
4c	δ	91.8	62.0	79.7	69.2	74.2	60.1	β-D-Man*p*2N	κN^2,O^3
	$\Delta\delta$	1.4	6.9	10.8	3.8	–1.2	0.3		
5	δ	104.5	65.7	80.0	75.4	74.2	60.6	β-D-Man*p*2N	κO^1,N^2:κ$O^{3,4}$
	$\Delta\delta$	14.1	10.6	11.1	10.0	–1.2	0.8		
6a	δ	100.5	56.8	68.6	68.1	70.8	61.2	α-D-Gal*p*2N	κO^1,N^2
	$\Delta\delta$	11.8	6.0	0.9	2.3	0.8	0.7		
6b	δ	103.0	61.3	72.3	67.9	76.7	61.1	β-D-Gal*p*2N	κO^1,N^2
	$\Delta\delta$	10.4	7.3	3.4	0.9	2.0	0.8		
6c	δ	91.7	57.2	76.1	70.1	70.8	61.2	α-D-Gal*p*2N	κN^2,O^3
	$\Delta\delta$	3.0	6.4	8.4	4.3	0.9	0.7		
6d	δ	95.9	61.2	80.1	70.5	76.5	60.9	β-D-Gal*p*2N	κN^2,O^3
	$\Delta\delta$	3.3	7.2	11.4	3.1	1.7	0.6		
6e	δ	108.3	67.8	75.4	82.6	71.2	63.2	α-D-Gal*f*2N	κO^1,N^2
7a	δ	99.6	59.9	77.5	77.3	69.0	61.5	α-D-Gal*p*2N	κO^1,N^2:κ$O^{3,4}$
	$\Delta\delta$	10.9	9.1	9.9	11.5	–0.9	1.0		
7b	δ	102.0	64.7	81.9	77.6	75.2	61.1	β-D-Gal*p*2N	κO^1,N^2:κ$O^{3,4}$
	$\Delta\delta$	9.4	10.7	13.0	10.6	0.4	0.8		

[a] Shifts in d^4-methanol ($\Delta\delta$ in parentheses): C1 103.0 (13.5), C2 72.9 (18.0), C3 82.4 (11.9), C4 75.6 (5.4), C5 73.1 (1.1), C6 61.2 (0.3). The assignment of the C2, C4 and C5 signal is uncertain.

to these four products, the signals of a fifth species were observed. This result made sense in light of the coordination behaviour of the parent glycoses, glucose and galactose. At the equimolar ratio, two pyranose chelators contributed to the major species for glucose (α- and β-κ$O^{1,2}$), whereas four well-developed chelators were provided by galactose: the pyranose κ$O^{1,2}$ chelators as found for glucose, the dominant furanose κ$O^{1,3}$ chelator, and a furanose κ$O^{1,2}$ chelator. Among these chelating diol moieties, the dominant furanose κ$O^{1,3}$ chelator was not expected to play a role for galactosamine since the amine function should be part of the chelate. The furanose κ$O^{1,2}$ chelator, however, should be expected, and, in fact, the spectroscopic data consistently pointed to a [Pd(en)(α-D-Gal*f*2N1H$_{-1}$-κO^1,N^2)]$^+$ species (**6e**). It should be noted that evidence for a furanose form of a glycosamine has been obtained for the first time here. For the major species of the equimolar Pd-en/Gal2N system, **6a**, a crystal-structure analysis supported the spectroscopically derived results. Pale yellow crystals of **6a**Cl·H$_2$O were obtained by allowing acetone vapours to diffuse into the aqueous reaction mixture. Fig. 3 shows the structure of the complex cation. The coordinated D-galactosamine exists in the favourable ^{4}C$_1$ conformation.

By repeating the reaction with a 2 : 1 molar ratio of Pd and D-galactosamine, the corresponding ^{13}C NMR spectra (Table 1, Fig. 2) indicated only the two anomers of [Pd$_2$(en)$_2$(D-Gal*p*2N1,3,4H$_{-3}$-κO^1,N^2:κ$O^{3,4}$)]$^+$ (**7a**, **b**) with a concomitant co-ordination at O1/N2 and O3/O4 (Scheme 3). In contrast to mono- and dimetallated glucosamine as well as to monometalled galactosamine, the β-pyranose of dimetallated galactosamine is the major species instead of the α-anomer. Tentatively, the reason could be a neighbouring-group effect of the 3,4-chelate. The axial 4-alkoxido ligand makes the O3 lone pairs turn in such a way that one comes into closer contact with a 2-amino hydrogen atom if the 1,2-chelate is diequatorial. However, calculations on the significance of this intramolecular hydrogen bond are outstanding.

As an interim result, a simplified picture can be drawn for palladium chelation by glycosamines in comparison to their parent glycoses since palladium(II) has a distinct preference for nitrogen instead of alkoxide ligators (note that the addition of en-type nitrogen chelators to solutions of palladium–glycose complexes liberates the glycose).[12] Thus, the mandatory inclusion of the 2-position into any chelate ring introduced a bias into the parent glycose's ligand set. In particular, the 1,3-furanose chelator—which provides the major ligand in the case of galactose—is missing, and 3,4-monometallation as observed for D-xylose and D-glucose is not observed.[11]

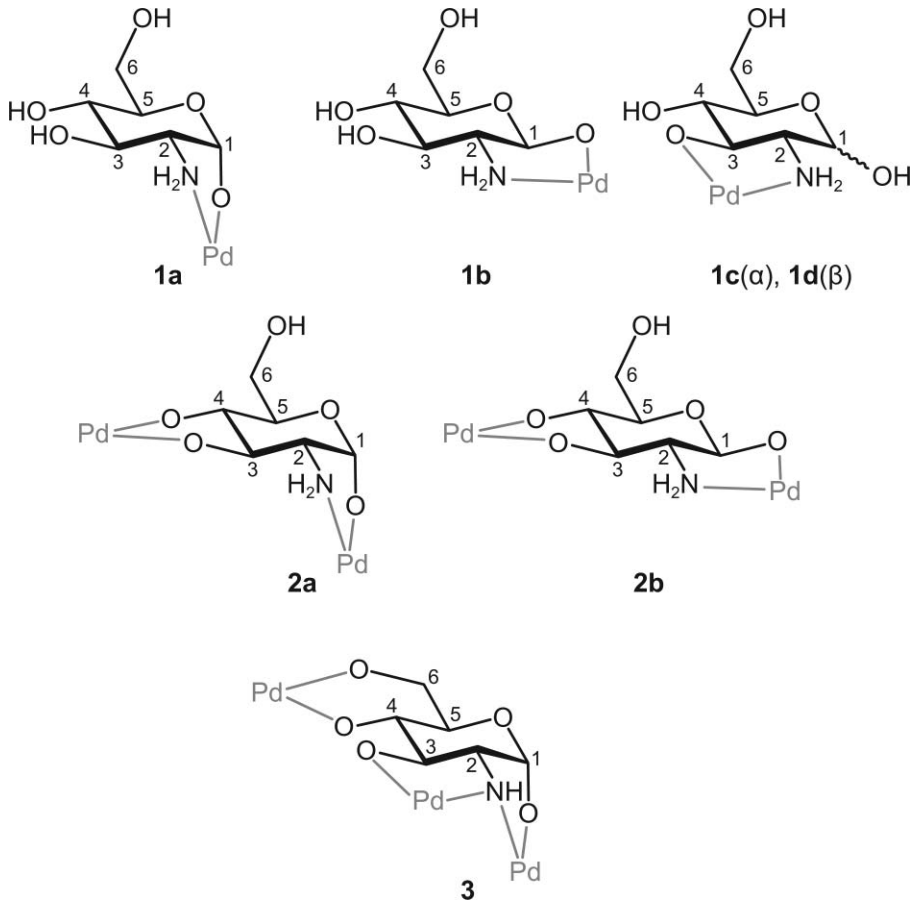

Scheme 1 The monocationic mono- (**1**) and dimetallated (**2**) D-glucosamine species detected in Pd-en (charges omitted), the grey symbol Pd denotes a Pd(en) moiety. A tentative formula **3** is given which is compatible with the chemical shifts observed for this species.

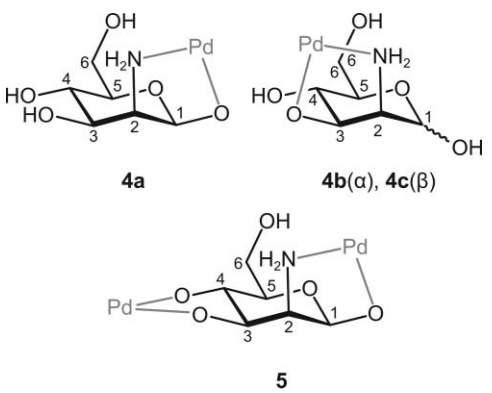

Scheme 2 The monocationic mono- (**4**) and dimetallated (**5**) D-mannosamine species detected in Pd-en. See Scheme 1 for abbreviations.

2-*N*-acetylamino-2-deoxy-glycose (*N*-acetylglycosamine) and 2-deoxy-glycose chelates

Although the coordination chemistry of the glycosamines may be considered complicated because of their configurational instability, their metal-binding O–C–C–N part is a known chelator.[14,15] Thus, it is not a question of whether the glycosamines form chelates but which individual isomers will contribute to which extent to the equilibria. The reverse holds true for the *N*-acetylaminoglycoses which, though they are ubiquitous and important biomolecules, are hardly considered ligands. The outcome of the work in this chapter will be that some isomers bind and some do not bind palladium centres through the acetylated amino function. In order to guide the reader through this chapter most conveniently, a rule will be introduced at the beginning which, in fact, emerged at a later stage of our investigation. This rule deals with the spatial requirements around the acetyl group. As will be seen from an X-ray analysis, the acetyl function, which is deprotonated on palladium chelation, adjusts itself almost coplanarly with the chelate ring. The region of space into which the acetyl function points has, of course, to be free of other substituents. Thus, Scheme 4 summarises yet-unobserved sterical arrangements which seem not to be permitted due to acetyl $\cdots$ hydroxyl repulsion.

In the non-permitted isomers, a pyranose's *N*-acetylamino function simply blocks the glycose's potentially metal-binding 2-position. In terms of its ligand properties, the 2-*N*-acetylamino-2-deoxy-D-glycopyranose thus resembles the respective 2-deoxy-D-glycopyranose that lacks any functional group at the 2-position.

It should be noted in the following section that in the class of 2-deoxy-aldohexoses, the lack of a 2-substituent reduces the number of eight aldohexoses to four 2-deoxy derivatives. 2-Deoxy-D-*lyxo*-hexose (*lyx*-dHex) is thus the 2-deoxy analogue of both D-galactose and D-talose, derivatives of the latter not being employed in this work. Accordingly, 2-deoxy-D-*arabino*-hexose (*ara*-dHex) is the 2-deoxy analogue of both D-glucose and D-mannose.

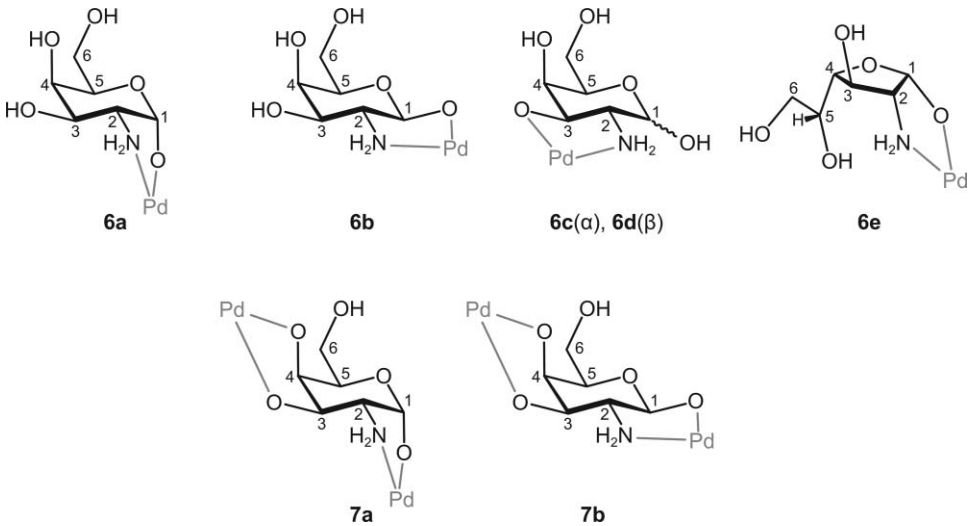

Scheme 3 The monocationic mono- (top) and dimetallated (bottom) D-galactosamine species detected in Pd-en. See Scheme 1 for abbreviations.

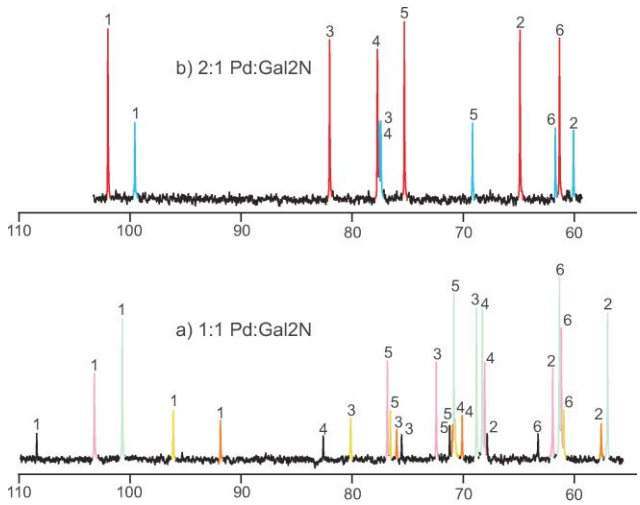

Fig. 2 ^{13}C NMR spectra of solutions of D-galactosamine hydrochloride in Pd-en. a) 1 : 1 molar ratio; light blue signals: the α anomer of $[Pd(en)(D\text{-}Gal\textit{p}2N1H_{-1}\text{-}\kappa O^1,N^2)]^+$ (**6a**), light red signals: the β anomer **6b**, orange signals: the α anomer of $[Pd(en)(D\text{-}Gal\textit{p}2N3H_{-1}\text{-}\kappa N^2,O^3)]^+$ (**6c**), yellowish signals: the β anomer **6d**., black signals: the α-furanose isomer $[Pd(en)(\alpha\text{-}D\text{-}Gal\textit{f}2N1H_{-1}\text{-}\kappa O^1,N^2)]^+$ (**6e**), b) 2 : 1 molar ratio; red signals: the β anomer of $[Pd_2(en)_2(D\text{-}Gal\textit{p}2N1,3,4H_{-3}\text{-}\kappa O^1,N^2\text{:}\kappa O^{3,4})]^+$ (**7b**), blue signals: the α anomer **7a**.

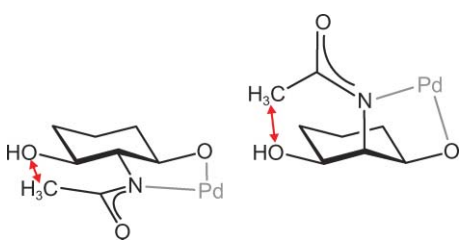

Scheme 4 Sterical arrangements that have not been observed for *N*-acetylaminoglycose–metal binding due to vicinal acetyl···hydroxyl repulsion. See Scheme 1 for abbreviations.

2-*N*-acetylamino-2-deoxy-D-glucose (*N*-acetyl-glucosamine, GlcNAc). As we know from its bonding to peptides, the palladium(II) centre is able to transform an amide function to a deprotonated amido ligand at a relatively low pH level.[16] The weakly acidic amide function of GlcNAc, in fact, reacts that way. Adding an equimolar amount of GlcNAc to Pd-en resulted in the formation of about eight species. In contrast, only two species made up the spectra if a 2 : 1 molar ratio of Pd : GlcNAc was adjusted. Fig. 4a shows the two signal sets. Keeping in mind the usual α/β anomerism of dimetallated D-glucopyranose and 2-amino-2-deoxy-D-glucopyranose, the two signal sets might have been interpreted to be indicative of this well-known type of isomerism. The generally small separation of the tentative

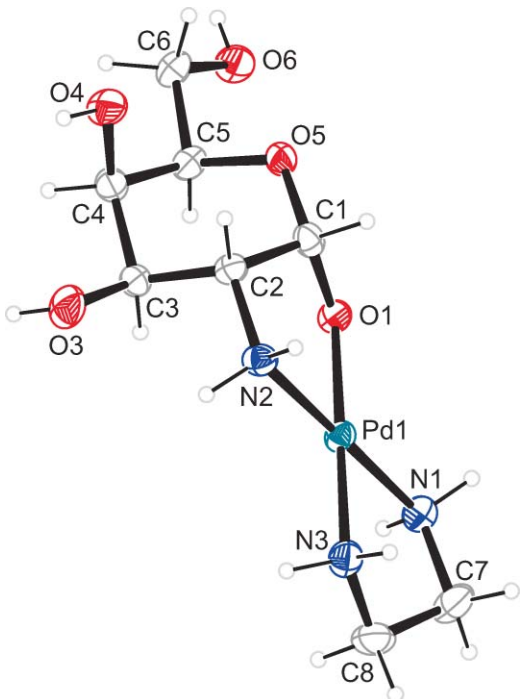

Fig. 3 Structure of the monocations in crystals of **6a**Cl·H_2O (50% probability ellipsoids). Distances [Å] and angles [°]: from Pd1 to: O1 2.016(3), N3 2.026(3), N2 2.034(3), N1 2.036(3); O1–Pd–N2 84.26(13), N3–Pd–N1 83.09(14); O1–C1–C2–N2 48.4(4), N1–C7–C8–N3 –52.8(5).

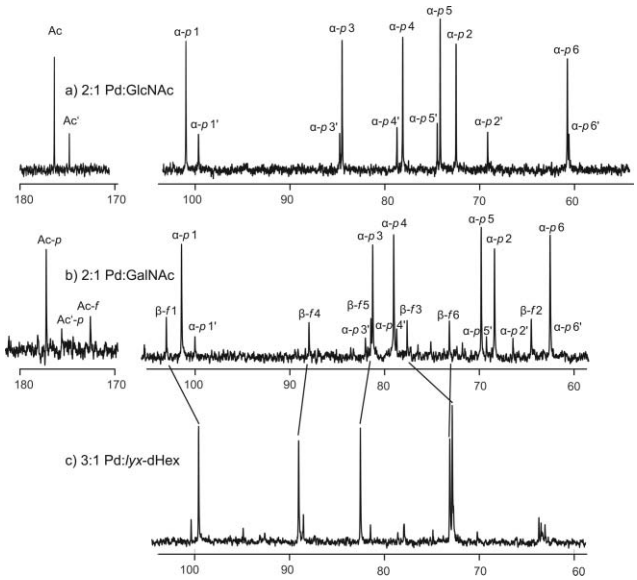

Fig. 4 a) ^{13}C NMR spectra (acetyl-CO and glucose signals shown, acetyl-Me signals mirror the carbonyl region) of solutions of GlcNAc in Pd-en at a molar 2 : 1 Pd : GlcNAc ratio; the two signal sets are assigned to acetyl isomers of [$Pd_2(en)_2$(α-D-Glc*p*2NAc1,2,3,4H$_{-4}$-κO^1,N^2:κ$O^{3,4}$)] (**9** and **9′** in Scheme 5). b) the same for GalNAc (**12a** and **12a′** in Scheme 6) which additionally formed the κ$O^{1,3}$:κ$O^{5,6}$-bonding β-furanose species **12b**. c) ^{13}C spectrum of a solution of *lyx*-dHex ("2-deoxy-galactose") in Pd-en at a molar 3 : 1 Pd : dHex ratio (C2 is outside the depicted ppm range, compare Table 2). All signals, except the five strongest of **13**, stem from minor monometallated species **11** (Scheme 6).

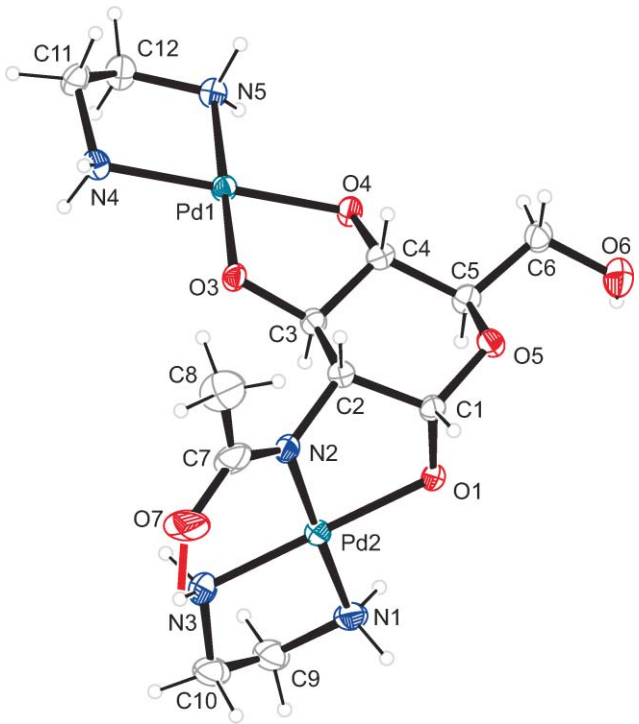

Fig. 5 Molecular structure of **9** in crystals of **9**·9.6H_2O (50% probability ellipsoids). Distances [Å] and angles [°]: from Pd1 to: O3 2.006(3), O4 2.021(3), N4 2.049(4), N5 2.052(3); Pd2 to: N2 2.002(4), N3 2.003(4), O1 2.003(3), N1 2.065(4); O1–Pd2–N2 83.4(2), O3–Pd1–O4 85.5(1); O1–C1–C2–N2 44.6(5), O3–C3–C4–O4 −57.4(4). The red bar denotes an intramolecular hydrogen bond [Å, °]: N3–H 0.92, H···O7 2.21, N3–H···O7 131, N3···O7 2.898(6).

anomers' signals, however, was irritating. Fortunately, signal assignment succeeded even for the minor species by means of 2D-NMR spectroscopy. Surprisingly, in terms of coupling constants as well as CIS values, both species were κO^1,N^2:κ$O^{3,4}$-dimetallated α-pyranoses instead of an a/β couple.

A hint towards the origin of the signal splitting came from an X-ray determination on yellow crystals that were grown from 2 : 1-type solutions. Although the crystals showed some degree of disorder among the water positions, the complex cations were well ordered. Fig. 5, in agreement with the NMR-spectroscopic result, shows an *N*-deprotonated amide function as a part of a κO^1,N^2 chelate. The environment of the amide-N atom is almost planar, the nitrogen lone pair thus having a mostly p character. The atomic distances indicate a delocalised double-bond character within the acetylamino function, which is thus expected to adopt one of two orientations that are coplanar with the chelate ring. Fig. 5 shows the obvious major isomer which is characterised by an intramolecular hydrogen bond from an ethylenediamine donor and the acetyl-O acceptor (N3–H···O7 in Fig. 5). It might be noted that Fig. 5 shows the first-ever determined crystal-structure analysis of a stable metal complex of the important biomolecule GlcNAc.

With this result, the species assignments in the GlcNAc solutions in Pd-en seem to make sense. The crystallised isomer is accompanied by the other, non-hydrogen-bonded and thus less stable acetyl isomer. According to this interpretation, the largest chemical-shift differences occurred for the C2 signals, followed by the signals of C1 and the acetyl-C(O). It should be noted as an interim result that, on the one hand, acetyl isomerism increases the number of solution species, and, on the other, a β anomer is not observed. To give a guess on the instability of the missing β anomer, the molecule of Fig. 5 and its β analogue, the latter as its hydrogen-bonded acetyl isomer, were calculated on the B3LYP/6-31G(d,p)/CEP-4G level of theory. As a result, the β isomer's acetyl group was tilted out of coplanarity with the chelate ring to minimise the repulsion to the 3-hydroxy function that is sketched in Scheme 4. In total, the sterically burdened β anomer was about 30 kJ mol^{-1} unstable with respect to the α form.

An analogous case was found at the 1 : 1 molar ratio. Here the major species (**8a** in Scheme 5) also came with a minor acetyl isomer whose individual ^{13}C NMR signals were not assigned. The tentative minor species **8b** and **8c** (Scheme 5) allowed us to hazard a guess on the driving force of acetamido ligation. In the parent hexose, glucose, both 2,3- and 3,4-diol chelation occured to a small extent.[11] In monometallated GlcNAc, however, the 2,3-chelator is suppressed although its α anomer is permitted by the above-mentioned rules. In conclusion, the acetylamido ligator was less available to a palladium(II) central atom, and the major chelate on monometallation was driven by the dominant O1 ligator.

2-*N*-acetylamino-2-deoxy-D-galactose (GalNAc) and 2-deoxy-D-*lyxo*-hexose (*lyx*-dHex). An aqueous solution of GalNAc consists of a major anomeric pyranose pair and a minor anomeric furanose pair in terms of ^{13}C NMR spectroscopy. The higher tendency of GalNAc to form furanoses remained on reaction with Pd-en. However, the ^{13}C NMR spectra of equimolar solutions were characterised by substantial signal overlap. Thus, a major

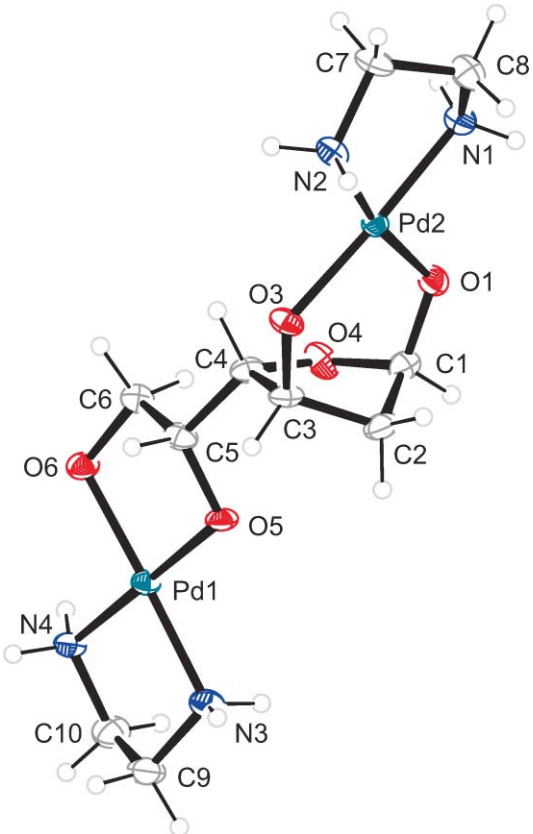

Fig. 6 Molecular structure of the *lyx*–dHex derivative **13** in crystals of **13**·8H_2O (70% probability ellipsoids). Distances [Å] and angles [°]: from Pd1 to: O5 2.012(2), O6 1.997(2), N3 2.045(2), N4 2.030(2); Pd2 to: O1 2.019(2), O3 2.023(2), N1 2.029(3), N2 2.042(3); O1–Pd2–O3 98.28(7), O5–Pd1–O6 85.99(7); O5–C5–C6–O6 45.5(3).

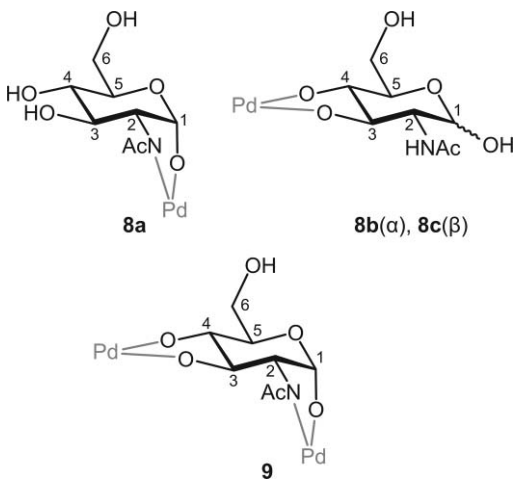

Scheme 5 **8a**: the major species of an equimolar solution of GlcNAc in Pd-en (two acetyl isomers observed, the minor species's ^{13}C NMR were not assigned). **8b**, **c**: the tentative minor species of the same solution (assignment of individual ^{13}C NMR signals failed). **9**: the only species in solutions of a molar 2 : 1 Pd : GlcNAc ratio (two acetyl isomers observed). See Scheme 1 for abbreviations.

[Pd(en)(α-D-Gal*p*2NAc1,2H$_{-2}$-κO^1,N^2)] (**10a**) as well as a minor anomeric couple of [Pd(en)(D-Gal*p*2NAc3,4H$_{-2}$-κ$O^{3,4}$)] (**10b**,**c**) seem reasonable in addition to about the same amount of free

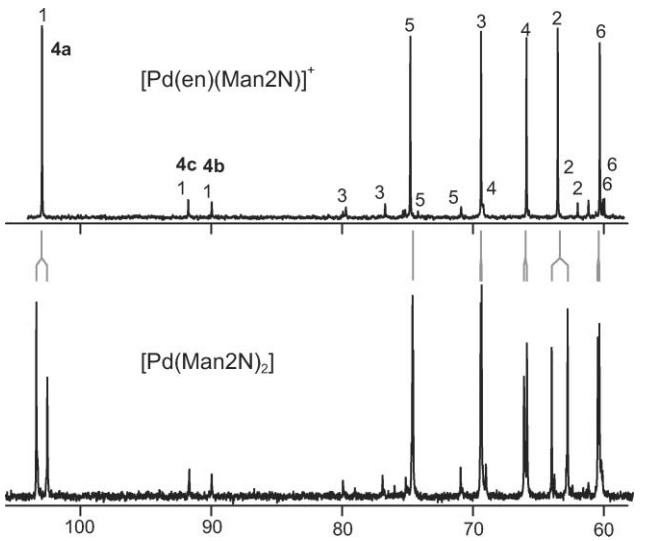

Fig. 7 Top: ^{13}C NMR spectrum of an equimolar solution of Man2N in Pd-en (Table 1). The species **4a–c** (Scheme 2) are assigned. Bottom: spectrum of a solution of a molar 2 : 1 ratio of Man2N·HCl and $[PdCl_4]^{2-}$ (4 equivalents hydroxide added). The main signals are split due to the *cis*/*trans* isomerism of the major κO^1,N^2:κO^1,N^2 species at the Pd centre.

GalNAc as detected for GlcNAc (Scheme 6). Moreover, the C1 and C4 regions point to the existence of furanoses. Better-resolved spectra were obtained for a 2 : 1 molar ratio of Pd and GalNAc (Fig. 4b). The major species is of the same kind as found for the glucose analogue and is identified as the dimetallated α-D-pyranose **12a** (Scheme 6). Again, a set of smaller signals accompanied the major species' signals that exhibit the typical spectroscopic trace of an acetyl isomer. As for the glucose derivative, a 1,2-metallated β isomer was neither expected from the above-mentoned rule (Scheme 4) nor actually observed. In contrast to GlcNAc, a third species of intermediate quantity was detected from the spectra of 2 : 1 batches (Fig. 4b). The typical C4 signal above 80 ppm pointed to a furanose ligand. Under the restrictions of galactose stereochemistry, two dimetallated furanose chelators are possible: α-furanose-κ$O^{1,2}$:κ$O^{5,6}$ which includes metal-binding by the 2-N atom and β-furanose-κ$O^{1,3}$:κ$O^{5,6}$ which does not. The NMR data pointed, however unconvincingly (due to cross-peak overlap in 2D spectra), to the latter isomer **12b** (Scheme 6). (The 1,2-bonding furanose species might be present in small quantities as indicated by the leftmost, unassigned signal in Fig. 4b). Since the κ$O^{1,3}$:κ$O^{5,6}$ ligand **12b** is the only possible galactose-derived bis(bidentate) chelator whose 2-function is not engaged in metal binding, an analogous species should be accessible with the related 2-deoxy derivative of galactose, 2-deoxy-D-*lyxo*-hexose.

The analysis of the metal-binding properties 2-deoxy-D-*lyxo*-hexose started with the aqueous solution equilibrium which showed a major anomeric pyranose pair as well as a minor anomeric furanose pair in terms of ^{13}C NMR spectra.[17] The addition of an equimolar amount of the Pd(en) probe made the free glycose almost vanish in favour of four metallated species. Adjustment to a 3 : 1 molar ratio of Pd : glycose showed that one of the four species was dimetallated and three were mononuclear complexes. Since well-resolved crosspeaks were, fortunately, obtained by applying 2D-NMR techniques to all employed metal : carbohydrate molar ratios, all four species were

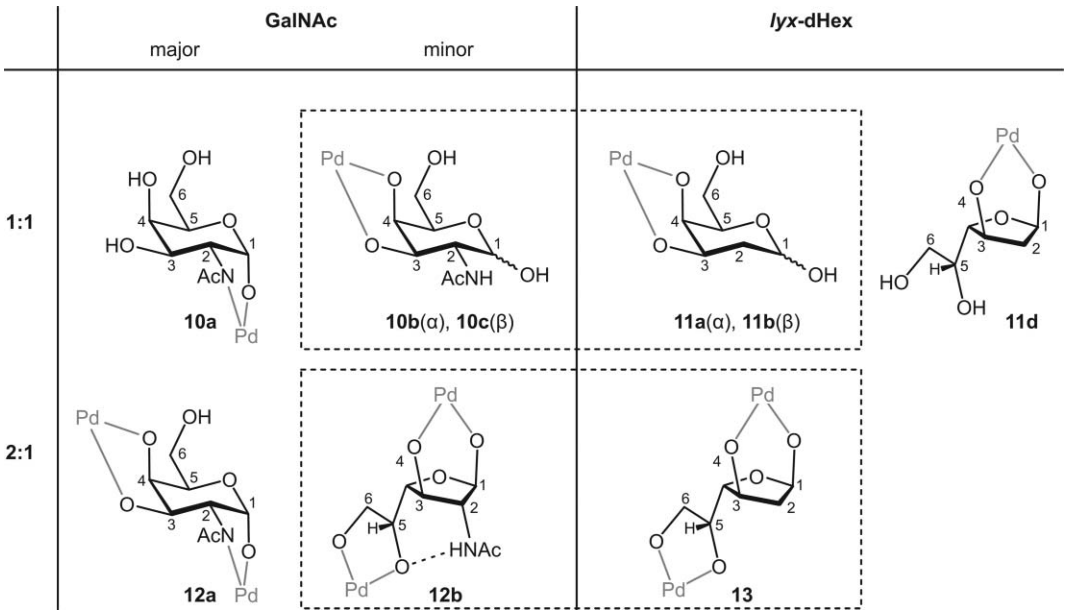

Scheme 6 GalNAc part, the major and minor Pd complexes at the specified molar ratios (the species in the left column form two acetyl isomers each; α/β anomerism is indicated by a wavy C1–O1 bond; the ^{13}C NMR signals of **10b** and **10c** were not assigned individually, the species thus being tentative). *lyx*-dHex part: the same for the related 2-deoxy glycose. The non-*N*-bonded GalNAc minor forms resemble the *lyx*-dHex major species (dashed boxes). See Scheme 1 for abbreviations.

identified (Table 2, Scheme 6). Fig. 4c shows the spectrum for the high metal : ligand ratio. As attempted by the stoichiometry, a sole dimetallated species (**13**) was observed (all minor species are monometallated).

The spectroscopic result was confirmed by single-crystal structure analysis. Fig. 6 shows the molecules of **13** in crystals of the octahydrate. We assumed an analogous structure for the *N*-acetylamino homologue (Scheme 6). In the scheme, a tentative intramolecular hydrogen bond is drawn in analogy to the parent galactofuranose complex.[18]

2-*N*-acetylamino-2-deoxy-D-mannose (ManNAc) and 2-deoxy-D-*arabino*-hexose (*ara*-dHex). The investigation of ManNAc shifted the focus definitively to furanose chelation even for the *N*-acetylamino derivatives. At a molar 2 : 1 ratio of Pd and ManNAc, a $\kappa O^1,N^2$-bonded pyranose was not detected. This result complies with the rule that an OH_{eq}–NAc–OH_{eq} moiety is unable to form such a chelate due to vicinal acetyl · · · hydroxyl repulsion. Keeping this rule in mind as well as the decreased preference of Pd^{II} centres for acetylated amino functions, the $\kappa O^{1,3}$:$\kappa O^{5,6}$ metallation pattern provided by the β-D-mannofuranose core (**15a**, Scheme 7), which ensures the bonding of the two offered palladium centres, gains importance. In fact, NMR-spectroscopic analysis consistently supports this assignment (Table 2). The dominant species **15a** was accompanied by a minor species which gave rise to a couple of signals in the C1 region. Consistent with what we had experienced throughout this work, this species should be **15b** as a couple of acetyl isomers. The rules retained their validity for equimolar mixtures of ManNAc in Pd-en. Spectrocopic analysis revealed the monometallated analogue of the furanose complex, [Pd(en)(β-D-Man*f*2NAc1,3H$_{-2}$-$\kappa O^{1,3}$)] (**14a**), as the major species, accompanied by four species of about the same concentration. Two of them were the anomeric pyranose mixture of unmodified ManNAc, the other two were, tentatively, assigned to an anomeric pair of 3,4-chelating pyranose, [Pd(en)(D-Man*p*2NAc3,4H$_{-2}$-$\kappa O^3,O^4$)] (**14b**,**c**, Scheme 7).

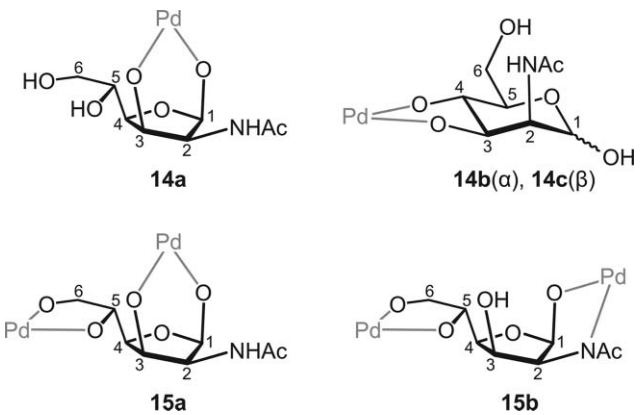

Scheme 7 **14a**: the major species in an equimolar solution of ManNAc in Pd-en. **14b**,**c**: tentative minor species. **15a**: the only assigned species at a molar 2 : 1 Pd : ManNAc ratio. **15b**: a tentative species which is based on a couple (= acetyl isomers) of minor signals at about 108 ppm in the ^{13}C NMR spectrum at a 2 : 1 molar ratio of Pd-en and ManNAc. See Scheme 1 for abbreviations.

Due to the exclusion of the sterically unsuitable *N*-acetylamino function from the major isomers in ManNAc's coordination chemistry, a close resemblance is expected between ManNAc and 2-deoxy-D-*arabino*-hexose. In fact, the major and only dimetallated species at a high Pd : glycose molar ratio was assigned to the binuclear β-D-furanose **17** (Scheme 8). The isomers that were formed at an equimolar ratio of palladium probe to *ara*-dHex closely parallel the results for the *lyx*-configured isomer. In both cases, monometallated 3,4-chelating pyranose as well as

Table 2 ^{13}C NMR shifts of 2-*N*-acetylamino-2-deoxy-glycose and 2-deoxy-glycose complexes in Pd-en (Pd-tmen for **16** and **17**). $\Delta\delta$, the difference of a shift in the presence of the metal probe and the free glycose derivative, is given if the values of the latter are accessible. Primed species denote minor acetyl isomers

		C1	C2	C3	C4	C5	C6	glycose isomer	chelating site
8a	δ	101.5	70.1	75.4	69.3	72.1	60.9	α-D-Glc*p*2NAc	$\kappa O^1,N^2$
	$\Delta\delta$	10.1	15.5	4.2	–1.3	0.1	–0.2		
9	δ	101.7	73.2	85.3	79.0	74.9	61.6	α-D-Glc*p*2NAc	$\kappa O^1,N^2:\kappa O^{3,4}$
	$\Delta\delta$	10.4	18.6	14.1	8.4	2.8	0.5		
9′	δ	100.4	69.9	85.5	79.6	75.2	61.4	α-D-Glc*p*2NAc	$\kappa O^1,N^2:\kappa O^{3,4}$
	$\Delta\delta$	9.1	15.3	14.3	9.0	3.1	0.3		
10a	δ	102.1	66.6	71.7	69.2	72.3	62.0	α-D-Gal*p*2NAc	$\kappa O^1,N^2$
	$\Delta\delta$	10.1	15.3	3.3	–0.4	0.9	–0.2		
11a	δ	92.6	35.8	73.8	78.6	70.3	63.4[c]	α-D-*lyx*-dHex*p*	$\kappa O^{3,4}$
	$\Delta\delta$	0.5	3.2	8.6	10.2	–1	1.1		
11b	δ	94.7	38.6	78	78	75	63.1[c]	β-D-*lyx*-dHex*p*	$\kappa O^{3,4}$
	$\Delta\delta$	0.2	3.2	9.4	10.7	–0.9	1.1		
11c	δ	100.4	[a]	72.9	88.6	72.8	63.8	β-D-*lyx*-dHex*f*	$\kappa O^{1,3}$
	$\Delta\delta$	1.4		[b]	3.2	[b]	0.2		
12a	δ	101.7	68.6	81.5	79.3	70.1	62.8	α-D-Gal*p*2NAc	$\kappa O^1,N^2:\kappa O^{3,4}$
	$\Delta\delta$	9.7	17.4	13.2	9.7	–1.4	0.6		
12b	δ	103.3	64.8	77.9	88.2	81.7	73.4	β-D-Gal*f*2NAc	$\kappa O^{1,3}:\kappa O^{5,6}$
	$\Delta\delta$	2.5	1.3	4.4	6.0	6.2	9.6		
13	δ	99.6	45.6	72.9	89	82.5	73.1	β-D-*lyx*-dHex*f*	$\kappa O^{1,3}:\kappa O^{5,6}$
	$\Delta\delta$	0.6	3.7	[b]	3.6	[b]	9.5		
14a	δ	97.1	57.5	70.1	81.3	71.9	64.5	β-D-Man*f*2NAc	$\kappa O^{1,3}$
14b	δ	94.4	56.5	79.1	75.7	75.5	61.5	α-D-Man*p*2NAc	$\kappa O^{3,4}$
	$\Delta\delta$	0.3	2.4	9.3	8.0	2.5	0.2		
14c	δ	94.9	56.7	83.5	75.9	77.7	61.6	β-D-Man*p*2NAc	$\kappa O^{3,4}$
	$\Delta\delta$	0.9	1.7	10.5	8.4	0.4	0.2		
15a	δ	96.1	56.6	69.4	82.9	79.0	74.3	β-D-Man*f*2NAc	$\kappa O^{1,3}:\kappa O^{5,6}$
16a	δ	101.2	[a]	71.5	82.2	73.1	64.7	β-D-*ara*-dHex*f*	$\kappa O^{1,3}$
16b	δ	92.2	40.4	78.0	81.5	75.2	[a]	α-D-*ara*-dHex*p*	$\kappa O^{3,4}$
	$\Delta\delta$	0.3	2.5	9.4	9.7	2.5			
16c	δ	95.1	42.4	81.5	81.5	77.0	[a]	β-D-*ara*-dHex*p*	$\kappa O^{3,4}$
	$\Delta\delta$	1.1	2.2	10.4	10.0	0.3			
17	δ	99.5	[a]	70.4	84.6	79.2	73.3	β-D-*ara*-dHex*f*	$\kappa O^{1,3}:\kappa O^{5,6}$

[a] signal coincides with signals of the palladium reagent [b] missing assignment of the free glycose [c] signals might be interchanged

1,3-metallated furanose isomers were observed. The origin of the unusual preference of the 3,4-site points to a property that is unique to the 2-deoxy glycoses and is not shared by the parent glycoses or by their amino and *N*-acetylamino derivatives. In all the 2-functionalised glycoses, the electron-withdrawing character of the 2-substituent contributes to the acidity of the 1-hydroxy function. For a Lewis acid of intermediate strength such as palladium(II), the ease of 1-deprotonation is the reason for the preferred contribution of O1 to metal bonding. In the 2-deoxy-glycoses, the acidity of the 1-hydroxy functions approaches that of the alcoholic functions. From the viewpoint of palladium(II) coordination, the absence of one, clearly more acidic, hydroxy function makes the 2-deoxy-glycoses different from the other glycoses and glycose derivatives.

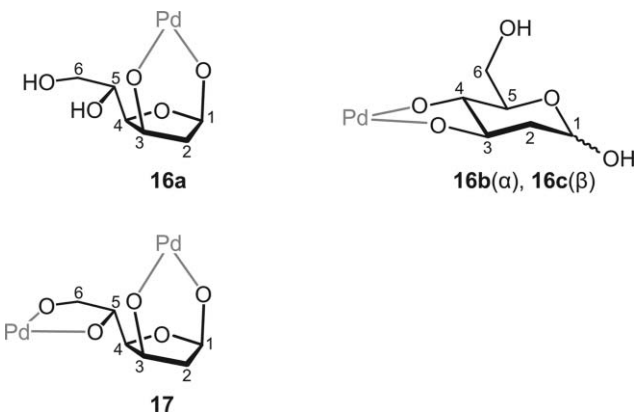

Scheme 8 **16a**: the minor monometallated furanose isomer of equimolar solutions of *ara*-dHex in Pd-tmen. **16b**,**c**: the major anomeric pair of monometallated pyranoses. **17** is the only dimetallated species at a threefold molar excess of palladium reagent over *ara*-dHex. See Scheme 1 for abbreviations.

Conclusions

In terms of their contribution to biochemical pathways and their availability as a renewable feedstock, the most important of the eight aldohexoses are D-glucose, D-mannose, and D-galactose. The same holds for their 2-modified derivatives, the 2-deoxy-2-amino-aldohexoses and the *N*-acetyl derivatives thereof, as well as for the 2-deoxy-aldohexoses. In particular, the *N*-acetylated glycosamines GlcNAc, ManNAc and GalNAc are ubiquitous biomolecules and the knowledge of their metal-binding properties should be a matter of course. Thus, keeping close to the palladium(II) centres of this work, a typical question that might be asked in the course of developing platinum(II) drugs might be whether or

not chelation of the Pt^{II} centres by, for example, GlcNAc has to be taken into account. Probing the bidentate metal-chelating sites of the 2-modified aldohexoses with $Pd^{II}N_2$ centres, some basic rules may be formulated. (1) Since the 2-modification does not affect the anomeric centre of the aldose, the 2-modified derivatives share the reducing property with their parent aldohexoses. This statement includes the fact that all the carbohydrates of this work are configurationally unstable and are able to enrich the most suitable chelator through their dynamic aqueous equilibrium which provides a pair of anomers of the furanose as well as the pyranose form. Each individual compound thus provides a ligand set similar to the set that has been found for the parent aldohexoses.[11] (2) The use of a palladium(II) probe implicates a preference of the central metal for nitrogen donors. The results obtained for the 2-deoxy-2-amino-glycoses complied with this experience. Thus no chelators with the 2-substituent dangling were found. Most notable, the well-developed 1,3-furanose chelator of galactose is missing. Instead, all the glycosamine isomers were bonded through N2. From the viewpoint of coordination chemistry, the evidence for a bridging amide ligand in **3**, which stems from an amine function that is deprotonated even in an aqueous environment, is remarkable. It should be noted, however, that this result deserves confirmation by solid-state work. (3) The chelating properties of the *N*-acetylated glycosamines are unexpected and follow special rules due to the stereochemical requirements of the acetyl function. Ruling out pyranose isomers that show enhanced acetyl $\cdots$ hydroxyl repulsion, the remaining isomers are well-suited chelators towards the employed palladium(II) probes. In other words: there *are* metal-binding sites at GlcNAc, ManNAc, and GalNAc. (4) The existence of "forbidden" *N*-acetyl-glycosamine chelation modes triggers the formation of competing chelators that have the 2-substituent dangling. The most prominent example is ManNAc whose coordination chemistry shows parallels to that of its 2-deoxy analogue, 2-deoxy-D-*arabino*-hexose. However, the 2-deoxy-glycoses also show a property that makes them unique among the reducing sugars. Since they are the only glycoses that lack an electron-withdrawing 2-substituent, their anomeric centre does not show the typical enhanced acidity that makes O1 usually contribute to the most stable chelate rings. Instead, the prominent palladium(II) chelators stem from the 3,4-chelating pyranose isomer.

In addition to these chemical rules, this work broadens our knowledge of the ^{13}C NMR trace of carbohydrate coordination. In particular the typical downfield 'coordination-induced' shifts may be useful to guess the metal-binding sites of derivatives of the chelators of this work. Examples include the above-mentioned work on the palladium(II)-binding sites of chitosan.[9,10] In the more recent contribution, coordination-induced ^{13}C NMR shifts are given for the 2,3-chelation of palladium(II) by a Glc2N-based β-glycoside. The numbers should be fairly close to those found for the β-D-Glc*p*2N complex **1d** of this work. However, there are marked deviations that may be helpful in a re-formulation of the more complicated bonding situation of oligosaccharide chelation.

In the introduction, platinum(II) chelation by the ligands of this work was shortly addressed. Work towards Pt^{II} analogues of the complexes reported herein is in progress. As an outlook, we can state as a prospect that there is spectroscopic evidence for the formation of related platinum compounds, but that the enhanced inertness of Pt^{II} complexes requires an individual approach.

Appendix: homoleptic glycosamine complexes

The glycosamine complexes of this work are heteroleptic. Interpretable spectroscopic results are assured by allowing a single glycose chelate at a palladium centre whose square-planar coordination is supplemented by a C_2-symmetric diamine spectator ligand (*i.e.*, *cis*/*trans* isomerism at the metal centre will not complicate the spectra). As expected, the situation becomes more complicated if the formation of homoleptic bis(glycosamine)palladium(II) complexes is attempted. Since each of the observed glycosamine isomers (*n*) may substitute the former spectator ligand, a total of $n(n + 1)$ complexes (including *cis*/*trans* isomers) might be expected. As a result, we expected hardly interpretable NMR spectra and they were. A proof that homoleptic complexes form at all is possible for the less chaotic case of Man2N. Since a single major species, the 1,2-chelating β-D-Man*p*2N isomer **4a**, was observed in equimolar batches of the Pd-en/Man2N system, the species distribution for an attempted $Pd(Man2N)_2$-type complex should be governed by the $Pd(\beta\text{-D-Man}p2N1H_{-1}\text{-}\kappa O^1,N^2)_2$ species. The ligand lacks C_2 symmetry, hence the signals of two major species, a *cis* and a *trans* isomer were expected. In agreement with the approximately 10% quantity of the minor isomers **4b** and **4c** in the Pd-en experiments, the next most abundant species in the homoleptic case were expected to be $\kappa O^1,N^2{:}\kappa N^2,O^3$-bonded in terms of chelator quantity. Fig. 7, in fact, shows all these details, including the expected extents of the splits that reflect the distance to the metal-binding site.

Experimental

Methods and materials

All chemicals were purchased and used without further purification. Reactions were carried out using standard Schlenk techniques in a nitrogen atmosphere.

NMR spectroscopy

Technical parameters. NMR spectra were recorded at room temperature on Jeol ECP 270 (^1H: 270 MHz, ^{13}C: 67.9 MHz, ^{31}P: 109 MHz), Jeol ECX 400/ECP 400 (^1H: 400 MHz, $^{13}C\{^1H\}$: 100 MHz, ^{31}P: 109 MHz) and Jeol ECP 500 (^1H: 500 MHz, $^{13}C\{^1H\}$: 125 MHz) spectrometers. Methanol was used as an internal standard for ^{13}C NMR spectra. Shift differences are given as $\delta(C_{complex}) - \delta(C_{free\ sugar})$. The values for the free glycose derivatives were taken from our own measurements in D_2O and were thus in neutral aqueous solution.

Species assignment. In the first step of species assignment, varying metal-to-carbohydrate molar ratios including free-ligand spectra were used to determine the number of metal centres bonded to a ligand. This technique has been described in detail in a glycose-directed work.[11] Various assignment levels were used for the metallated species. In terms of cross-peak overlap, a species was characterised by means of 2-dimensional techniques, if possible. In these cases, assignment of individual signals including $^3J_{H,H}$ coupling constants and the application

of Karplus relationships allowed the determination of a ligand's configuration and conformation (furanose or pyranose, α or β anomer, $^4C_1$ or $^1C_4$ pyranose chair).[19,20] The metal-binding site was determined afterwards and showed (5-membered chelate rings), or not (6-membered chelate rings), a typical down-field shift of those carbon atoms that bear metal-binding oxygen atoms: the so-called coordination-induced shift (CIS). As a rule, all the major species were confirmed following this procedure. Conclusions regarding species that did not allow a 2D-based treatment were drawn on the basis of their ^{13}C NMR signal pattern. On this assignment level, furanoses (δ_{C4} about 80–85 ppm) and pyranoses (no CIS-corrected signals in this region) have been reliably distinguished. In order to assess the total number of species including non-identified minor species, the number of signals in the C1 region of the ^{13}C NMR spectra (*ca.* 95–110 ppm) was indicative. Lastly, tentative species assignments were made on the basis of the signals in the C1 region.

^{1}H NMR (400 MHz, D_2O) data

δ (ppm) (sp. = superposed): **6a**: 5.12 (d, 1H, *H1*,$^3J_{1,2}$ = 3.7 Hz), 4.28 (dd, 1H, *H3*,$^3J_{3,4}$ = 3.1 Hz), 3.85 (dd, 1H, *H5*, $^3J_{4,5} \approx {}^3J_{5,6} \approx$ 6.3 Hz), 3.77 (d, 1H, *H4*), 3.50 (sp., 2H, *H6a/b*), 2.67 (dd, 1H, *H2*, $^3J_{2,3}$ = 10.6 Hz). **6b**: 4.30 (d, 1H, *H1*,$^3J_{1,2}$ = 8.1 Hz), 3.61–3.47 (sp., 5H, *H3*, *H4*, *H5*, *H6a/b*), 2.39 (dd, 1H, *H2*, $^3J_{2,3}$ = 10.8 Hz). **6d**: 4.45 (d, 1H, *H1*,$^3J_{1,2}$ = 7.9 Hz), 3.25 (sp., 1H, *H3*), 3.61–3.47 (sp., 5H, *H3*, *H4*, *H5*, *H6a/b*), 2.45 (sp., 1H, *H2*). **6e**: 5.05 (d, 1H, *H1*,$^3J_{1,2}$ = 3.7 Hz), 4.49 (t, 1H, *H3*, $^3J_{2,3} = {}^3J_{3,4}$ = 5.5 Hz), 3.66 (sp., 1H, *H4*), 3.04 (dd, 1H, *H2*).

8a: 4.87 (d, 1H, *H1*, $^3J_{1,2}$ = 3.7 Hz), 4.39 (dd, 1H, *H3*,$^3J_{2,3}$ = 9.5 Hz, $^3J_{3,4}$ = 9.7 Hz), 3.58 (sp., 1H, *H5*), 3.56 (sp., 2H, *H6a/b*), 3.26 (dd, 1H, *H4*, $^3J_{4,5}$ = 9.0 Hz), 2.96 (dd, 1H, *H2*).

9: 4.64 (d, 1H, *H1*, $^3J_{1,2}$ = 3.5 Hz), 4.33 (t, 1H, *H3*,$^3J_{2,3} = {}^3J_{3,4}$ = 9.5 Hz), 3.55–3.35 (sp., 3H, *H5*, *H6a/b*), 2.81 (dd, 1H, *H2*), 2.77 (t, 1H, *H4*, $^3J_{4,5}$ = 9.5 Hz). **9′**: 4.94 (dd, 1H, *H3*,$^3J_{2,3}$ = 9.5, $^3J_{3,4}$ = 9.7 Hz), 4.49 (d, 1H, *H1*, $^3J_{1,2}$ = 3.5 Hz), 3.55–3.35 (sp., 4H, *H2*, *H5*, *H6a/b*), 2.85 (t, 1H, *H4*, $^3J_{4,5}$ = 9.5 Hz).

11a: 1.78 (dd, 1H, *H2a*, $^2J_{2a,2b}$ = 12.9 Hz, $^3J_{2a,3}$ = 5.5 Hz), 2.44 (m, 1H, *H2b*), 3.31–3.34 (sp., 1H, *H3*), 3.61 (m, 1H, *H4*), 3.86 (m, 1H, *H5*), 5.36 (dd, 1H, *H1*, $^3J_{1,2a} < 1$ Hz, $^3J_{1,2b}$ = 3.3 Hz).

11b: 1.85–1.91 (sp., 1H, *H2a*), 2.16–2.23 (m, 1H, *H2b*), 3.13–3.18 (m, 1H, *H3*), 3.44–3.47 (sp., 1H, *H5*), 3.52–3.56 (sp., 1H, *H4*), 4.62 (dd,1H, *H1*, $^3J_{1,2a} < 1$ Hz, $^3J_{1,2b}$ = 8.5 Hz). **11c**: 1.46 (d, 1H, *H2a*, $^3J_{2a,2b}$ = 12.9 Hz, $^2J_{2a,3} < 1$ Hz), 1.95–2.00 (m, 1H, *H2b*, $^3J_{2b,3}$ = 5.0 Hz), 3.39 (d, 1H, *H3*, $^3J_{3,4} < 1$ Hz), 3.52–3.56 (sp., 1H, *H5*), 3.98 (d, 1H, *H4*, $^3J_{4,5}$ = 3.6 Hz), 4.76 (d, 1H, *H1*, $^3J_{1,2a} < 1$, $^3J_{1,2b}$ 4.4 Hz).

12a: 4.83 (sp., 1H, *H1*), 3.78 (sp., 1H, *H3*), 3.74 (sp., 1H, *H5*), 3.65 (dd, 1H, *H2*, $^3J_{1,2}$ = 3.5 Hz, $^3J_{2,3}$ = 9.2 Hz), 3.61 (dd, 1H, *H4*, $^3J_{3,4} \approx {}^3J_{4,5} \approx$ 4.1 Hz), 3.38 (sp., 2H, *H6a/b*).

13: 1.40 (d, 1H, *H2a*, $^2J_{2a,2b}$ = 13.2 Hz, $^3J_{2a,3} < 1$ Hz), 1.86–1.91 (m, 1H, *H2b*, $^3J_{2b,3}$ = 4.7 Hz), 3.06 (dd, 1H, *H6a*, $^2J_{6a,6b}$ 9.3 Hz), 3.19–3.23 (m, 1H, *H6b*), 3.23–3.28 (m, 1H, *H5*, $^3J_{5,6a}$ = 3.0 Hz), 3.33 (d, 1H, *H3*, $^3J_{3,4} < 1$ Hz), 3.95 (d, 1H, *H4*, $^3J_{4,5}$ = 5.5 Hz), 4.69 (d, 1H, *H1*, $^3J_{1,2a} < 1$ Hz, $^3J_{1,2b}$ = 4.4 Hz).

14a: 4.77 (sp., 1H, *H5*), 4.37 (d, 1H, *H1*, $^3J_{1,2}$ = 4.4 Hz), 3.84–3.79 (sp., 2H, *H2*, *H6a*), 3.40 (sp., 1H, *H4*), 3.32 (sp., 1H, *H3*). **14b**: 4.69 (s, 1H, *H1*), 3.95 (sp., 1H, *H2*), 3.65–3.55 (sp., 2H, *H6a/b*), 3.50 (sp., 1H, *H5*), 3.45 (sp., 1H, *H3*), 3.32 (sp., 1H, *H4*). **14c**: 4.65 (s, 1H, *H1*), 4.06 (sp., 1H, *H2*), 3.62–3.56 (sp., 1H, *H6a*), 3.42–3.38 (sp., 1H, *H6b*), 3.34 (sp., 1H, *H3*), 3.03 (sp., 1H, *H5*), 2.98 (sp., 1H, *H4*).

15a: 4.49 (sp., 1H, *H5*), 4.28 (d, 1H, *H1*,$^3J_{1,2}$ = 4.6 Hz), 3.76 (t, 1H, *H2*, $^3J_{2,3} \approx {}^3J_{3,4} \approx$ 4.6 Hz), 3.45–3.41 (sp., 2H, *H4*, *H6a*), 3.27 (sp., 1H, *H6b*), 3.21 (sp., 1H, *H3*).

16a: 3.71–3.75 (sp., 1H, *H5*), 4.59 (dd, 1H, *H1*, $^3J_{1,2a}$ = 4.5 Hz). **16b**: 1.48–1.52 (m, 1H, *H2a*), 1.91 (m, 1H, *H2b*, $^2J_{2a,2b}$ = 12.4 Hz), 2.78–2.90 (sp., 1H, *H4*), 3.57–3.61 (sp., 1H, *H3*), 3.67–3.71 (sp., 1H, *H5*), 5.12 (m, 1H, *H1*). **16c**: 1.28–1.34 (m, 1H, *H2a*), 1.97–2.00 (m, 1H, *H2b*), 2.78–2.90 (sp., 1H, *H4*), 3.22–3.25 (m, 1H, *H5*), 3.39–3.46 (sp., 1H, *H3*), 4.70 (m, 1H, *H1*).

17: 1.99 (m, 1H, *H2a*), 3.34 (dd, 1H, *H6a*, $^2J_{6a,6b}$ = 10.2 Hz), 3.40–3.44 (m, 1H, *H3*, $^3J_{3,4}$ = 2.8 Hz), 3.53 (dd, 1H, *H6b*), 3.79 (dd, 1H, *H4*, $^3J_{4,5}$ = 9.1 Hz), 4.52 (d, 1H, *H1*, $^3J_{1,2a}$ = 4.7 Hz), 4.53–4.56 (m, 1H, *H5*, $^3J_{5,6a}$ = 5.8 Hz, $^3J_{5,6b}$ = 3.6 Hz).

DFT calculations

DFT calculations were performed using the B3LYP method implemented in Gaussian 03.[21] The CEP-4G basis was used for palladium, the 6-31G(d,p) basis for the ligand atoms.

Synthesis

The Pd-based reagents Pd-en and Pd-tmen were prepared following published procedures.[22] Their nomenclature was introduced in prior work, Pd-en thus being an aqueous solution of ethylenediamine-dihydroxido-palladium(II), [Pd(en)$(OH)_2$] of specified concentration. In Pd-tmen, *N,N,N′,N′*-tetramethylethylenediamine replaces the en ligand.[12] A general procedure for the reaction of the Pd reagents was applied to glycosamine hydrochlorides, *N*-acetyl-glycosamines and 2-deoxy-hexoses. Under ice cooling and nitrogen, 0.1–0.3 mmol of the glycose derivative was dissolved in an equimolar, twofold or threefold amount of the Pd reagent (*circa* 0.3 M solution in D_2O). The yellow solutions were stirred for some hours under ice cooling prior to the NMR measurement. All reaction mixtures could be stored at −60 °C for further use.

Crystals were prepared for three compounds: **6a**Cl·H_2O: D-galactosamine-hydrochloride (55 mg, 0.26 mmol) was dissolved in 0.30 M Pd-en (0.85 mL, 0.26 mmol) and stirred for 20 h. Light yellow crystals (10 mg, 0.03 mmol,10%) were obtained within two months by diffusion of acetone vapor into the solution. **9**·9.6H_2O: *N*-acetyl-D-glucosamine (33 mg, 0.15 mmol) were dissolved in 0.30 M Pd-en (1.0 mL, 0.30 mmol) and stirred for 20 h. Light yellow crystals (30 mg, 0.04 mmol, 26%) were obtained within two days by diffusion of acetone vapor into the solution. **13**·8H_2O: 2-deoxy-D-*lyxo*-hexose (25 mg, 0.15 mmol) was dissolved in 0.30 M Pd-en (1.0 mL, 0.30 mmol) and stirred for 20 h. Light yellow crystals (24 mg, 0.04 mmol, 25%) were obtained within two days by diffusion of acetone vapor into the solution.

Single-crystal X-ray methods

Details of the crystal-structure analyses are collected in Table 3.

Table 3 Crystal-structure analyses

	6aCl·H_2O	**9**·9.6H_2O	**13**·8H_2O
net formula	$C_8H_{22}ClN_3O_6Pd$	$C_{12}H_{39}N_5O_{15.57}Pd_2$	$C_{10}H_{40}N_4O_{13}Pd_2$
M_r/g mol^{-1}	398.15	715.58	637.28
Crystal size/mm	0.10 × 0.035 × 0.025	0.29 × 0.26 × 0.16	0.18 × 0.11 × 0.07
T/K	200(2)	200(2)	100(3)
Radiation	Mo-Kα	Mo-Kα	Mo-Kα
Diffractometer	KappaCCD	XCalibur	XCalibur
Crystal system	Orthorhombic	Orthorhombic	Monoclinic
Space group	$P2_12_12_1$	$P2_12_12_1$	$P2_1$
a/Å	5.1253(2)	16.4419(14)	10.12039(15)
b/Å	10.9658(3)	7.6517(7)	8.54783(12)
c/Å	24.5604(8)	21.4470(11)	12.89436(19)
β (°)	90	90	91.7968(13)
V/Å^3	1380.37(8)	2698.2(4)	1114.91(6)
Z	4	4	2
D_c/g cm^{-3}	1.91587(11)	1.7616(3)	1.89836(10)
μ/mm^{-1}	1.564	1.406	1.679
Absorption correction	multi-scan	multi-scan	analytical
Transmission factor range	0.936–0.962	0.90398–1.00000	0.7865–0.8901
Refls. measured	7354	11351	12615
R_{int}	0.0378	0.0296	0.0254
Mean $\sigma(I)/I$	0.0591	0.0437	0.0351
θ range	3.72–27.57	3.75–26.28	3.69–27.53
Observed refls.	2812	4748	4664
x, y (weighting scheme)	0.0108, 0.6746	0.0326, 1.3550	0.0210, 0
Hydrogen refinement	mixed	mixed	mixed
Flack parameter	–0.02(3)	–0.02(3)	–0.049(19)
Refls in refinement	3160	5215	5137
Parameters	181	348	311
Restraints	3	18	25
$R(F_{obs})$	0.0325	0.0315	0.0207
$R_w(F^2)$	0.0652	0.0711	0.0436
S	1.042	1.049	0.991
Shift/error$_{max}$	0.001	0.002	0.001
Max electron density/e Å^{-3}	0.538	0.554	0.861
Min electron density/e Å^{-3}	–0.426	–0.513	–0.431

Acknowledgements

The authors thank Martin Steinborn for computer-chemical work on metallated GlcNAc isomers. Sandra Albrecht is acknowledged for technical assistance. This work was supported by the Deutsche Forschungsgemeinschaft (grant Kl 624/12-1).

References

1 J. Lerivrey, B. Dubois, P. Decock, G. Micera, J. Urbanska and H. Kozlowski, *Inorg. Chim. Acta*, 1986, **125**, 187–190.
2 E. V. Isaeva, A. M. Agranovich, N. A. Dobrynina, L. I. Martynenko, A. M. Evseev and V. I. Spitsyn, *Bull. Acad. Sci. USSR, Div. Chem. Sci. (Engl. Transl.)*, 1987, **36**, 864–866.
3 J. Urbanska, H. Kozlowski, A. Delannoy and J. Hennion, *Anal. Chim. Acta*, 1988, **207**, 85–94.
4 S. Bunel, C. Ibarra, E. Moraga, V. Calvo, A. Blaskó and C. A. Bunton, *Carbohydr. Res.*, 1993, **239**, 185–196.
5 E. Ferrari and M. Saladini, *J. Inorg. Biochem.*, 2004, **98**, 1002–1008.
6 S. Bunel, C. Ibarra, E. Moraga, A. Blaskó and C. A. Bunton, *Carbohydr. Res.*, 1993, **244**, 1–14.
7 S. Bunel, C. Ibarra, E. Moraga, J. Parada, A. Blasko, C. Whiddon and C. A. Bunton, *Carbohydr. Res.*, 1998, **312**, 191–200.
8 H. Junicke, Y. Arendt and D. Steinborn, *Inorg. Chim. Acta*, 2000, **304**, 224–229.
9 N. V. Kramareva, A. Y. Stakheev, O. P. Tkachenko, K. V. Klementiev, W. Grünert, E. D. Finashina and L. M. Kustov, *J. Mol. Catal. A: Chem.*, 2004, **209**, 97–106.
10 S. A. Johannesen, B. O. Petersen, J. O. Duus and T. Skrydstrup, *Inorg. Chem.*, 2007, **46**, 4326–4335.
11 Y. Arendt, O. Labisch and P. Klüfers, *Carbohydr. Res.*, 2009, **344**, 1213–1224.
12 R. Ahlrichs, M. Ballauff, K. Eichkorn, O. Hanemann, G. Kettenbach and P. Klüfers, *Chem.–Eur. J.*, 1998, **4**, 835–844.
13 D. Horton, J. S. Jewell and K. D. Philips, *J. Org. Chem.*, 1966, **31**, 4022–4025.
14 W. Plass, *Coord. Chem. Rev.*, 2009, **253**, 2286–2295.
15 A. Singh and R. C. Mehrotra, *Coord. Chem. Rev.*, 2004, **248**, 101–118.
16 C. G. Ágoston, T. K. Jankowska and I. Sóvágó, *J. Chem. Soc., Dalton Trans.*, 1999, 3295–3302.
17 S. J. Angyal, *Carbohydr. Res.*, 1994, **263**, 1–11.
18 P. Klüfers and T. Kunte, *Chem.–Eur. J.*, 2003, **9**, 2013–2018.
19 C. A. G. Haasnoot, F. A. A. M. de Leeuw and C. Altona, *Tetrahedron*, 1980, **36**, 2783–2792.
20 A. Navarro-Vazquez, J. C. Cobas, F. J. Sardina, J. Casanueva and E. Diez, *J. Chem. Inf. Comput. Sci.*, 2004, **44**, 1680–1685.
21 M. J. Frisch, G. W. Trucks, H. B. Schlegel, G. E. Scuseria, M. A. Robb, J. R. Cheeseman, J. A. Montgomery, T. Vreven, K. N. Kudin, J. C. Burant, J. M. Millam, S. S. Iyengar, J. Tomasi, V. Barone, B. Mennucci, M. Cossi, G. Scalmani, N. Rega, G. A. Petersson, H. Nakatsuji, M. Hada, M. Ehara, K. Toyota, R. Fukuda, J. Hasegawa, M. Ishida, T. Nakajima, Y. Honda, O. Kitao, H. Nakai, M. Klene, X. Li, J. E. Knox, H. P. Hratchian, J. B. Cross, V. Bakken, C. Adamo, J. Jaramillo, R. Gomperts, R. E. Stratmann, O. Yazyev, A. J. Austin, R. Cammi, C. Pomelli, J. W. Ochterski, P. Y. Ayala, K. Morokuma, G. A. Voth, P. Salvador, J. J. Dannenberg, V. G. Zakrzewski, S. Dapprich, A. D. Daniels, M. C. Strain, O. Farkas, D. K. Malick, A. D. Rabuck, K. Raghavachari, J. B. Foresman, J. V. Ortiz, Q. Cui, A. G. Baboul, S. Clifford, J. Cioslowski, B. B. Stefanov, G. Liu, A. Liashenko, P. Piskorz, I. Komaromi, R. L. Martin, D. J. Fox, T. Keith, A. Laham, C. Y. Peng, A. Nanayakkara, M. Challacombe, P. M. W. Gill, B. Johnson, W. Chen, M. W. Wong, C. Gonzalez and J. A. Pople, Gaussian, Inc., Wallingford, 2004.
22 K. Gilg, T. Mayer, N. Ghaschghaie and P. Klüfers, *Dalton Trans.*, 2009, 7934–7945.